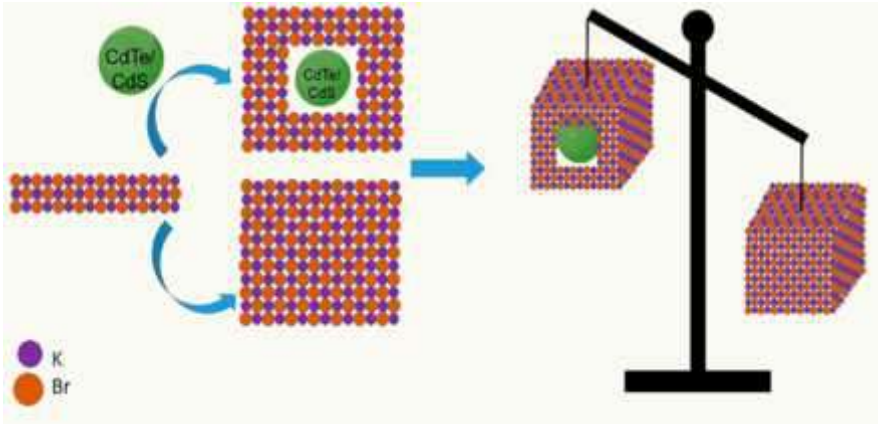

Fig. Scheme of salt and salt:QDs composite crystal growth: 1 - center of crystallization, 2 - incorporation of nanoparticles into the crystal (violet – K^+cations, red – Br^- anions and green – CdTe/CdS nanoparticles (to scale), 3 – comparison of salt and composite crystal density.

In this research work, we suggest, that QDs are not closely packed into the composite crystal so some pores are formed and this causes the decrease of the density of KBr:CdTe/CdS composite comparing to the pure salt crystal.

Panasenko N. V.

SYNTHESIS AND FLUORESCENCE SPECTRUM OF 9-(4-PYRAZOLYL) DECAHYDROACRIDINDIONES-1,8

Department of Medical and Pharmaceutical Chemistry
Bukovinian State Medical University

One of the most important problems of modern photoelectronics is the purposeful creation of materials with predetermined physical properties. To create liquid crystal displays, you need dyes not only with certain optical characteristics, but also quite stable under prolonged UV irradiation.

Recently, dyes of decahydroacridine structure have been studied in detail, as they are promising, from the point of view of practical application, as laser materials and fluorescent labels in biological objects. Such materials have highly efficient phototransformation processes.

To construct complex and promising decahydroacridinediones-1,8 with a pyrazole nucleus at position 9, we developed the synthesis conditions and studied their absorption and luminescence spectra depending on the electronic nature of the substituents in the 1st and 3rd positions of the pyrazole nucleus.

The basic synthons for the synthesis of the target hybrid compounds 4 were 1,3-disubstituted 4-pyrazolecarbaldehydes 1, dimedone 2 and ammonium acetate in ethyl alcohol.

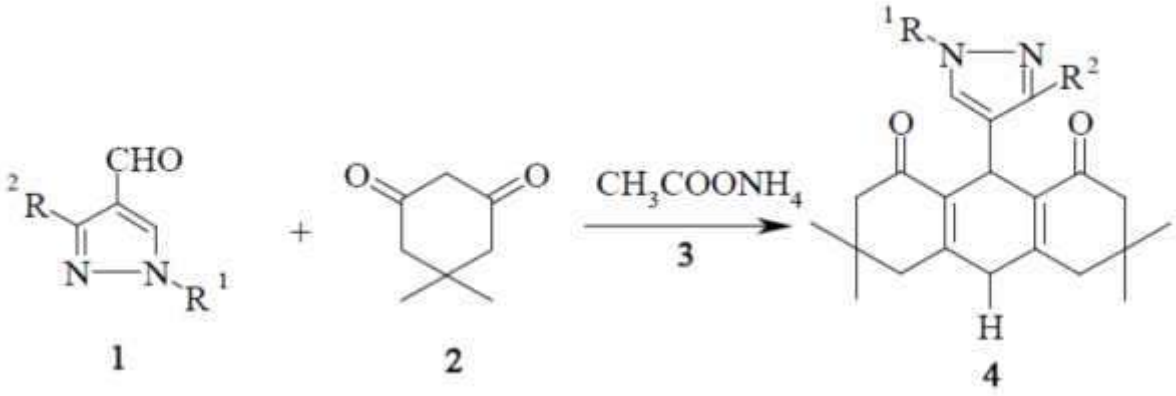

R^1= CH_3, CH_2CH_2CN, CH_2CH_2COOH, C_6H_5

R^2 = COOH, $COOC_2H_5$, C_6H_4 , 4-MeC_6H_4 , 4-$MeOC_6H_4$ 3- pyridyl, 4- pyridyl , 2- thienyl, 2-benzofuryl.

The composition of the obtained compounds was reliably confirmed by elemental analysis and mass spectrometry, and the structure was established by NMR spectroscopy.

The absorption spectra of compounds 4 are quite similar with a pronounced band in the range of 330-450 nm and an intense band in the range of 240-320 nm. The fluorescence spectra of the target compounds are monoband. The band practically does not change when the wavelength of excitation changes. Quantum fluorescence yields were measured relative to coumarin.

The highest quantum yield of 23 % has a compound containing a methyl group in position 1 and a carboxyl group in position 3 of the pyrazole nucleus.

Tkachuk M.M.

RESEARCH OF THE NON-EQUILIBRIUM OF THE DIFFUSE LAYER FOR THE DESCRIPTION OF THE ELECTROCHEMICAL KINETICS NEAR THE ROTATING DISK ELECTRODE BY NUMERICAL SOLUTIONS OF THE STRICT BOUNDARY PROBLEM

Department of Medical and Pharmaceutical Chemistry
Bukovinian State Medical University

The Frumkin's theory of electrochemical kinetics contains an assumption about the Boltzmann distribution of concentrations in the diffuse layer of electroactive components. However, these studies on the restrictions on the use of this model have not yet been made to the end. The Frumkin's fundamental theory of electrode reactions (with the Boltzmann distribution of concentrations in the diffuse layer) and the model based on a numerical solution of equations of stationary multicomponent diffusion near the rotating disk electrode (RDE) are compared with each other. The simulation was carried out using tested numerical methods and Mathcad program. The strict boundary problem of the mass transfer near the RDE includes:

1. The equation of material balance, taking into account the mechanisms of transfer of matter due to diffusion, migration, convection and homogeneous reaction with the participation of the electroactive substance:

$$\frac{\partial c_i}{\partial t} = -\nabla \vec{J}_i + R_i,\ \vec{J}_i = -D_i \nabla c_i - D_i \frac{z_i F}{RT} c_i \nabla \varphi + \vec{V} c_i,\ \text{i=1,...,n;} \qquad (1)$$

2. The equation of potential distribution near the charged electrode surface:

$$\nabla^2 \varphi = -F / \varepsilon \cdot \varepsilon_0 \sum_{k=1}^{n} z_i c_i \qquad (2)$$

3. The solution of stationary hydrodynamic equations for systems with the working RDE:

$$\vec{V} = V_\varphi \vec{e}_\varphi + V_r \vec{e}_r + V_x \vec{e}_x, \qquad (3)$$

where $\vec{e}_\varphi, \vec{e}_r, \vec{e}_x$ - normed basic vectors in the orthogonal cylindrical coordinate system;

$V_\varphi(x,\varphi) = \varphi \mu F(\xi); V_x(x) = \sqrt{\nu\mu} H(\xi);\ V_r(x,\varphi) = \varphi \mu G(\xi);\ \xi = x\sqrt{\mu/\nu}$; a=-0,51023; b=-0,61602;

$F(\xi) = a\xi - \xi^2/2 - 1/3 b\xi^3 + \ldots$; $G(\xi) = 1 + b\xi + 1/3 a\xi^3 + \ldots$; $H(\xi) = -a\xi^2 + 1/3\xi^3 + b/6\P^4 \ldots$;.

4. To describe an electrical double layer, the Gouy-Chapman-Stern-Grahame model is used. For z-z valence background electrolyte, the potential dependence from the distance within the diffuse layer ($x_d \le x_i$) is given by the equation:

$$\varphi(x_i) = \frac{RT}{F} \cdot \frac{4}{|z|} \cdot ath\left(exp[-\frac{(x_i - x_d)}{a}] \cdot th\left(\frac{|z|\varphi_2}{4} \cdot \frac{F}{RT} \right) \right), \qquad (4)$$

5. The dependence of potential from distance within a Stern layer ($0 < x_i \le x_d$) can be calculated as:

$$\varphi(x_i) = \varphi_m - (\varphi_m - \varphi_2) \cdot x_i / x_d, \qquad (5)$$

where φ_m is the value of the metallic surface potential (x=0).

6. The connection between the potential of the electrode, measured relative to the potential of zero charge φ_0 and the potential jump in the diffuse layer φ_2 is expressed through the ratio of integral capacities of Stern K_{02} and diffuse K_2 layers:

$$\frac{\varphi_0}{\varphi_2} = 1 + \frac{K_2}{K_{02}},\quad \frac{\varphi_{02}}{\varphi_2} = \frac{K_2}{K_{02}},\quad \frac{K_2(\varphi_2)}{K_{02}(\varphi_2)} = \frac{\varepsilon \cdot \varepsilon_0}{K_{02}(\varphi_2) \cdot a} \cdot sh\left(\frac{|z|F}{2RT} \varphi_2 \right) \Big/ \frac{|z|F}{2RT} \varphi_2. \qquad (6)$$